

# Full-band and atomistic simulation of n- and p-doped double-gate MOSFETs for the 22nm technology node

Mathieu Luisier and Gerhard Klimeck

Network for Computational Nanotechnology, Purdue University, West Lafayette, IN 47907, USA

E-mail: mluisier@purdue.edu

**Abstract**—Physics-based simulations are widely recognized as an helpful support to develop novel transistor structures. In this paper we describe a two-dimensional full-band and atomistic simulator. The  $sp^3d^5s^*$  tight-binding model is used as bandstructure model. Our tool allows the treatment of realistically extended n- and p-doped double-gate field-effect transistors. The devices are designed according to the ITRS specifications for the 22 nm technology node. Different crystal and surface orientations are investigated and compared to the ITRS targets. The importance of including spin-orbit coupling in the bandstructure model is discussed for p-doped FETs.

## I. INTRODUCTION

Double-gate metal-oxide-semiconductor field-effect transistors (DG MOSFETs) are promising candidates to replace the conventional planar bulk MOSFETs starting at the 22 nm technology node in 2012. Since the fabrication of novel devices is always a difficult and expensive process physics-based simulation tools can support their development. This field is known as technology computer aided design (TCAD).

The theoretical investigation of DG MOSFETs has attracted a lot of attention in the recent years. Different kind of approaches have been proposed. Among them we can cite the work of Z. Ren et al. [1] which is based on an effective mass and mode space Non-Equilibrium Green's Function approach, of A. Svizhenko et al. [2] who solved the same problem, but in real-space, of D. Mamaluy et al. [3] who improved the calculation of the device-contact coupling, or of S. Laux et al. [4] which relies on the Quantum Transmitting Boundary Method. Full-band and atomistic approaches have also been proposed, but on a one-dimensional and semi-classical level[5] or for very small device dimensions and primitive bandstructure models[6].

Here, we study realistic n- and p-doped Si MOSFETs using an atomistic and full band simulator based on the semi-empirical  $sp^3d^5s^*$  tight-binding method. The dimensions and supply voltages of the devices are chosen

as suggested by the ITRS for the 22 nm node[7]. Among other properties the surface orientation and the transport direction of DG MOSFETs are very important since they profoundly affect their current characteristics. This issue is addressed in this paper for the three most important configurations experimented in the industry, (a) surface orientation along the (100) crystal axis and transport along the  $\langle 100 \rangle$  axis, (b) surface along the (110) axis with  $\langle 110 \rangle$  oriented channel, and finally (c) surface along the (111) axis and transport in the  $\langle 112 \rangle$  direction.

## II. METHOD

To simulate DG MOSFETs as shown in Fig. 1 a two-dimensional full-band Schrödinger-Poisson is sufficient. In effect the third dimension (in plane  $z$ -axis) is assumed periodic so that the density-of-states  $g(x, y, E, k_z)$  and the transmission through the structure  $T(E, k_z)$  depend on two spectral variables, the injection energy  $E$  into the device and the wave vector  $k_z$  that models the third dimension. Carrier  $n(x, y)$  and current  $I_d$  densities are calculated by integrating the density-of-states and transmission over the entire contact Brillouin Zone

$$n(x, y) \propto \sum_{C=L,R} \sum_{k_z} \int dE g^C(x, y, E, k_z) \cdot f^C(E)$$
$$I_d \propto \sum_{k_z} \int dE T(E, k_z) \cdot (f^R(E) - f^L(E)).$$

The sum over the variable  $C$  represents the contribution from the left ( $L$ ) and right ( $R$ ) reservoirs where a Fermi distribution  $f^{L,R}(E)$  of the electrons is assumed.

The nearest-neighbor  $sp^3d^5s^*$  tight-binding method is used as bandstructure model since it allows a correct description of the electron and hole characteristics[8]. Thus, the anisotropy of the Si bandstructure as illustrated in Fig. 2 is fully taken into account in the transport model. Spin-orbit coupling is neglected for electrons since it is weak in Si devices[9], but taken into account for the hole transport. To calculate the position dependent density-of-states and transmission coefficients of the

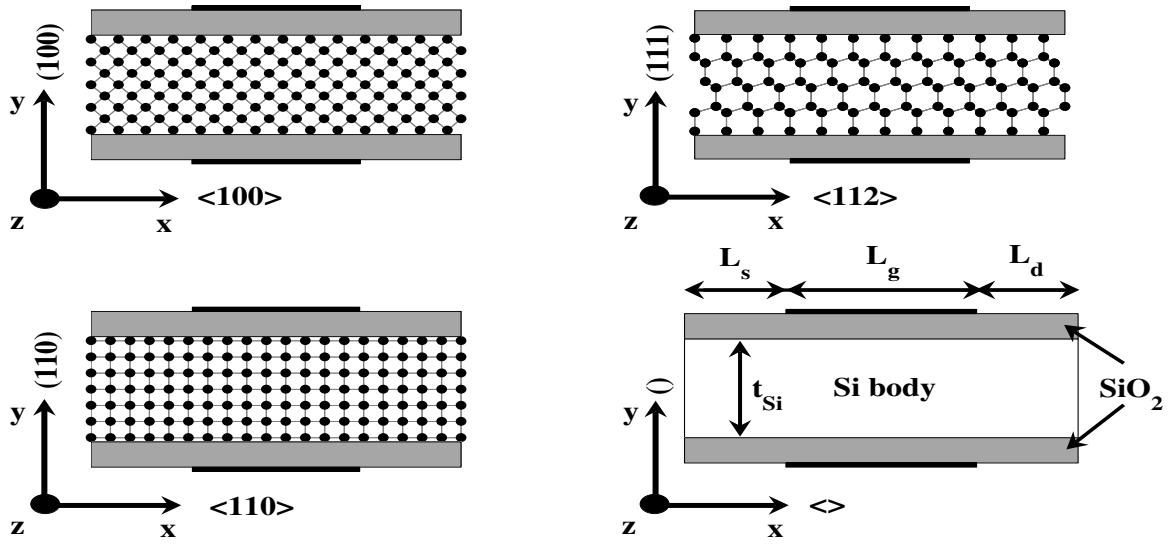


Fig. 1. Schematic view of double-gate field-effect transistors with different surface orientations  $y$  labeled  $()$  and transport directions  $x$  labeled  $\langle \rangle$ . In all the structures the  $\text{SiO}_2$  oxide layers (gray) have a thickness  $t_{ox}=1.3$  nm, the Si body  $t_{Si}=4.9$  nm, the gate length  $L_g$  measures 22 nm, the source  $L_s$  and drain  $L_d$  extensions 10 nm. The source and drain are doped with  $N_D=10^{20}$   $\text{cm}^{-3}$  ( $N_A=10^{20}$   $\text{cm}^{-3}$ ) in n- (p-) MOSFETs.

DG MOSFETs we use an approach equivalent to the Non-Equilibrium Green's Function formalism, but more efficient in the case of ballistic transport[10] and that can be easily parallelized[11]. The 2D Poisson equation is solved on a finite-element grid by assuming point charges on each atom constituting the transistor structure.

### III. RESULTS

We consider n- and p-doped DG MOSFETs designed along the ITRS specifications for the 22 nm technology node[7], i. e. gate length  $L_g=22$  nm, equivalent oxide thickness  $\text{EOT}=1.3$  nm ( $\text{SiO}_2$  layers), power supply voltage  $V_{dd}=\pm 1$  V. The work function of the metal gate contacts ( $\phi_M=4.6$  eV) is chosen so that the threshold voltage of the n- (p-) doped transistors lies around 440 (-470) meV. The source and drain contacts are doped with  $N_{D,A}=10^{20}$   $1/\text{cm}^3$  donors or acceptors. The body thickness of the transistors is set to  $t_{Si}=4.9$  nm. It is large enough so that eventual surface roughness effects and process variations have a limited influence on the simulation results.

The current characteristics  $I_d - V_{gs}$  at  $V_{ds} = \pm V_{dd}$  of the different DG MOSFETs depicted in Fig. 1 are shown in Fig. 3 and some important quantities like ON-current, threshold voltage, and subthreshold swing are summarized in Fig. 4. The electron currents do not

include spin-orbit coupling, the hole currents do. The ITRS requires a OFF-current of  $1e-5$   $\mu\text{A}/\mu\text{m}$  and a ON-current of  $673$   $\mu\text{A}/\mu\text{m}$  for DG transistors at the 22 nm technology node. The three device structures fulfill these criteria with a considerable margin. However, it is worth noting that in reality the intrinsic ON-current is deteriorate by the voltage drop caused by the source and drain access resistances and the OFF-current is increased by gate leakage mechanisms. These effects are not taken into account in this study. They would require a multi-scale simulation approach where the contact regions are modeled in a classical way and the active part of the transistor on a quantum mechanical level.

According to bulk experimental data[12] the (100)/ $\langle 100 \rangle$  configuration offers the highest (lowest) electron (hole) mobility, followed by (111)/ $\langle 112 \rangle$ , and finally (110)/ $\langle 110 \rangle$ . Keeping the dimensions and the threshold voltage constant, the device with the highest mobility exhibits the highest ON-current. Hence the experimental trends are confirmed by our simulation results for the ON-current, as shown in Fig. 3 and 4.

The spin-orbit splitting energy has a value of 45 meV in silicon. Consequently, this effect is not important for electron transport. However, it is not clear whether it plays a crucial role or not in the transport properties of holes. For this reason we compare in Fig. 5 the

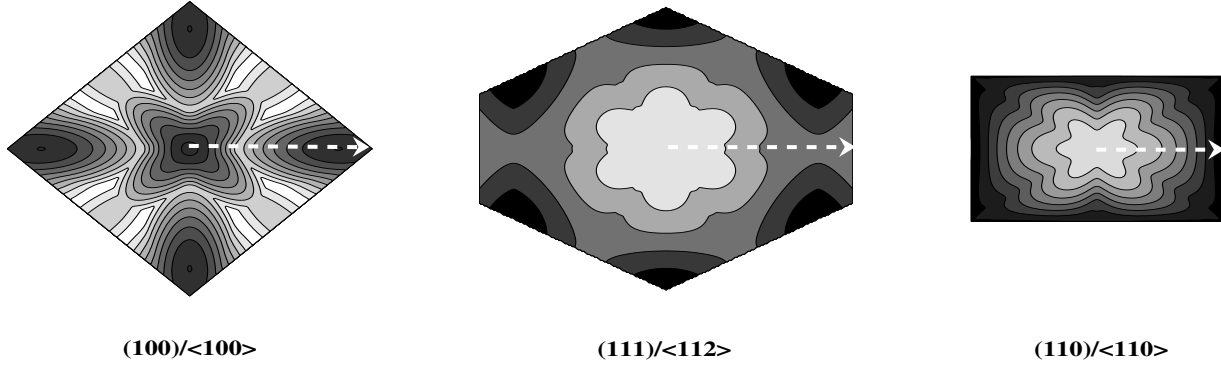


Fig. 2. Contour plot of the bandstructure of the semi-infinite source and drain extensions in the first Brillouin Zone for the (100) surface orientation (left, lowest conduction subband), the (111) surface (middle, highest valence subband), and the (110) surface (right, highest valence subband). White arrows depict the transport directions labeled  $\langle \rangle$ .

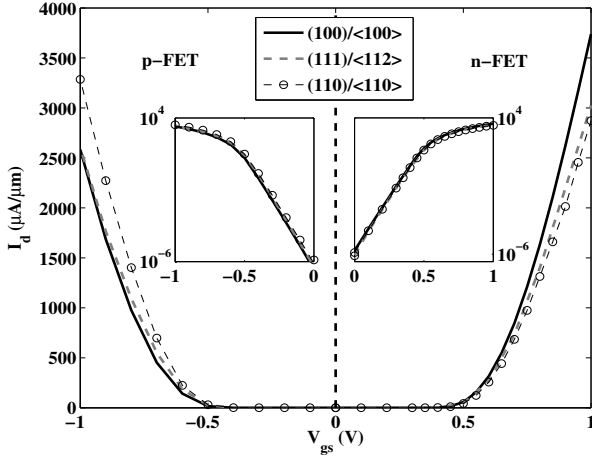


Fig. 3. Linear and logarithmic (insets) transfer characteristics  $I_d - V_{gs}$  of p- (left) and n- (right) doped double-gate FETs at  $V_{ds} = \pm V_{DD}$ . The currents of the three transistor configurations schematized in Fig. 1 are shown. All simulations are done at room temperature (spin-orbit coupling only for the pFETs).

		(100)	(111)	(110)
		$\langle 100 \rangle$	$\langle 112 \rangle$	$\langle 110 \rangle$
n	$I_{ON}$ (mA/ $\mu\text{m}$ )	3.74	3.02	2.87
	$I_{OFF}$ ( $\mu\text{A}/\mu\text{m}$ )	1.8e-6	8.5e-7	1.3e-6
	$V_{th}$ (mV)	450	440	440
	$S$ (mV/dec.)	63	64	63
p	$I_{ON}$ (mA/ $\mu\text{m}$ )	2.58	2.6	3.29
	$I_{OFF}$ ( $\mu\text{A}/\mu\text{m}$ )	2.8e-7	4.5e-7	7.6e-7
	$-V_{th}$ (mV)	480	460	470
	$S$ (mV/dec.)	63	63	64

Fig. 4. ON-current  $I_{ON}$  ( $I_{ON}=I_d$  at  $V_{ds}=V_{gs}=\pm V_{DD}$ ,  $V_{DD}=1.0$  V), OFF-current  $I_{OFF}$  ( $I_{OFF}=I_d$  at  $V_{ds}=\pm V_{DD}$ ,  $V_{gs}=0$  V), threshold voltage  $V_{th}$ , and sub-threshold swing  $S$  of the three n- (upper part of the table, no spin-orbit coupling) and p-doped (lower part, spin-orbit coupling included) FETs simulated in this work.

hole current of the three device configurations with and without spin-orbit coupling. It is found that the threshold voltage and the subthreshold swing are not affected by the absence of spin-orbit coupling. The (100)/ $\langle 100 \rangle$  device has a ON-current that is 7% higher when spin-orbit coupling is included, no change is observed for (111)/ $\langle 112 \rangle$ , and spin-orbit coupling decreases the current of the (110)/ $\langle 110 \rangle$  structure by 4.8%.

A comparison of the transmission coefficients (at  $V_{ds}=V_{gs}=-1$  V) with and without spin-orbit coupling is shown in Fig. 6 for the (100)/ $\langle 100 \rangle$  p-FET. The first

current channels open earlier in the case of spin-orbit coupling leading to a higher drain current. This energy offset is smaller for the two other device configurations, especially for the (111)/ $\langle 112 \rangle$  pFET where spin-orbit effects can be neglected.

#### IV. CONCLUSION

In this paper we demonstrated a full-band and atomistic simulator dedicated to DG MOSFETs with arbitrary surface orientation and transport direction. Compared to previous full-band simulations of similar structures[6] we add a more comprehensive bandstructure model ideal for

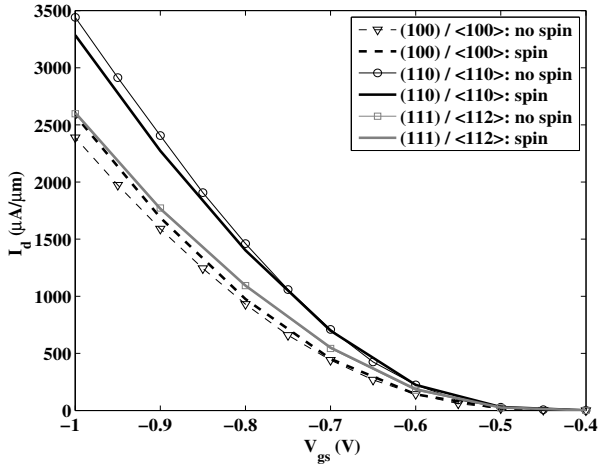


Fig. 5. Comparison of the transfer characteristic  $I_d - V_{gs}$  ( $V_{ds} = -1$  V) with spin-orbit coupling (lines without symbols) and without (lines with symbols) of the p-doped FETs in Fig. 1.

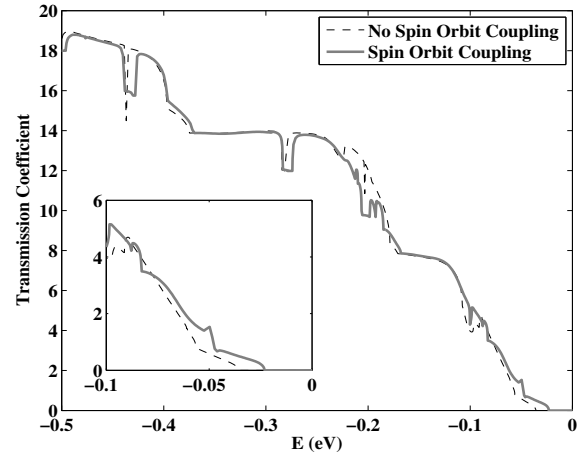


Fig. 6. Transmission coefficient through the (100)/<100> pFET at  $V_{ds} = V_{gs} = -1$  V. The gray line refers to results with spin-orbit coupling, the dashed line without.

electrons and holes, we are able to simulate devices with realistic dimensions, including spin-orbit coupling, and we can reproduce experimental trends.

#### ACKNOWLEDGMENT

This work was partially supported by NSF grant EEC-0228390 that funds the Network for Computational Nanotechnology, by NSF PetaApps grant number 0749140, and by NSF through TeraGrid resources provided by the Texas Advanced Computer Center (TACC) and Indiana University (IU). TeraGrid systems are hosted by Indiana University, LONI, NCAR, NCSA, NICS, ORNL, PSC, Purdue University, SDSC, TACC and UC/ANL. nanohub.org computer resources were also used.

#### REFERENCES

- [1] Z. Ren, R. Venugopal, S. Goasguen, S. Datta, and M. S. Lundstrom, "nanoMOS 2.5: A Two-Dimensional Simulator for Quantum Transport in Double-Gate MOSFETs", *IEEE Trans. Electron. Dev.*, vol. 50, 1914, 2003.
- [2] A. Svizhenko, M. P. Anantram, T. R. Govindan, R. Biegel, and R. Venugopal, "Two-dimensional quantum mechanical modeling of nanotransistors", *J. Appl. Phys.*, vol. 91, 2343, 2002.
- [3] D. Mamaluy, M. Sabathil, and P. Vogl, "Efficient method for the calculation of ballistic quantum transport", *J. Appl. Phys.*, vol. 93, 4628, 2003.

- [4] S. E. Laux, A. Kumar, and M. V. Fischetti, "Ballistic FET modeling using QDAME: quantum device analysis by modal evaluation", *IEEE Transactions On Nanotechnology*, vol. 1, 255, 2002.
- [5] A. Rahman, G. Klimeck, and M. S. Lundstrom, "Novel Channel Materials for Ballistic Nanoscale MOSFETs-Bandstructure Effect", *IEDM Tech. Digest*, p. 605, 2005.
- [6] H. Minari and N. Mori, "Atomistic modeling of hole transport in ultra-thin body SOI pMOSFETs", to appear in the *J. of Comp. Elec.*, available at <http://www.springerlink.com/content/j50664u6ptw10704/>, 2008.
- [7] <http://www.itrs.net>
- [8] T. B. Boykin, G. Klimeck, and F. Oyafuso, "Valence band effective-mass expressions in the  $sp^3d^5s^*$  empirical tight-binding model applied to a Si and Ge parametrization", *Phys. Rev. B*, vol. 69, 115201, 2004.
- [9] M. Luisier and A. Schenk, "Atomistic Simulation of Nanowire Transistors", *J. of Comp. and Theor. Nanoscience*, vol. 5, 1031, 2008.
- [10] M. Luisier, G. Klimeck, A. Schenk, and W. Fichtner, "Atomistic Simulation of Nanowires in the  $sp^3d^5s^*$  Tight-Binding Formalism: from Boundary Conditions to Strain Calculations", *Phys. Rev. B*, vol. 74, 205323, 2006.
- [11] T. B. Boykin, M. Luisier, and G. Klimeck, "Multi-band transmission calculations for nanowires using an optimized renormalization method", *Phys. Rev. B*, vol. 77, 165318, 2008.
- [12] B. Mereu, C. Rossel, E. P. Gusev, and M. Yang, "The role of Si orientation and temperature on the carrier mobility in metal oxide semiconductor field-effect transistors with ultra-thin HfO2 gate dielectrics", *J. of Appl. Phys.*, vol. 100, 014504, 2006.